Physics – Uspekhi **55** (8) 808 – 837 (2012)

CONFERENCES AND SYMPOSIA

PACS numbers: 01.10.Fv, **04.20. – q**, **04.70. – s**, 47.27.Gs, 47.35.Pq, 68.03.Kn, 72.25.Hg, 72.25.Pn, 72.25.Rb, **71.35. – y**, 73.63.Hs, **78.47. – p**, **78.67. – n**, **96.50. – e**, **96.60. – j**, **95.75. – z**, **98.80. – k**

Modern problems in the physical sciences
(Scientific session of the Physical Sciences Division of the Russian Academy of Sciences, 30 November 2011)

DOI: 10.3367/UFNe.0182.201208f.0869

On 30 November 2011, a scientific session of the Physical Sciences Division of the Russian Academy of Sciences (RAS) was held in the conference hall of the Lebedev Physical Institute, RAS.

The agenda of the session announced on the RAS Physical Sciences Division website www.gpad.ac.ru included the following reports:

(1) **Ivchenko E L** (Ioffe Physical Technical Institute, RAS, St. Petersburg) "Spin physics in semiconductor nanosystems";

(2) **Golub L E** (A F Ioffe Physical Technical Institute, RAS, St. Petersburg) "Spin transport in heterostructures";

(3) **Levchenko A A** (Institute of Solid State Physics, RAS, Chernogolovka, Moscow region) "Capillary turbulence on the surface of quantum liquids";

(4) **Babin S A** (Institute of Automation and Electrometry, Siberian Branch of the RAS) "New generation modes in fiber lasers";

(5) **Kurt V G** (Astro-Space Center of the Lebedev Physical Institute, RAS, Moscow) "Motion of the Sun through the interstellar medium";

(6) **Lukash V N** (Astro-Space Center of the Lebedev Physical Institute, RAS, Moscow) "Cosmological flow generation in general relativity".

Papers written on the basis of oral reports 1–3, 5, and 6 are presented below.

PACS numbers: **71.35. – y**, **78.47. – p**, **78.67. – n**
DOI: 10.3367/UFNe.0182.201208g.0869

Spin physics in semiconductor nanosystems

E L Ivchenko

1. Introduction

The rapid development of nanotechnologies in the past two decades has aroused sustained interest in semiconductor spin physics (see Refs [1–3] for a review). The driving factor behind this interest is the paradigm of using spin, an additional degree of freedom of an electron, as a tool for the quantum processing of information. In classical computing, the basic unit of information is a bit, which, regardless of its particular physical realization, takes one of the two mutually exclusive values, either 0 or 1 (yes/no, yin or yang, etc.). A qubit (q-bit, or quantum bit), similar to a bit, admits two eigenstates, $|0\rangle$ and $|1\rangle$. The difference between the bit and the qubit is fundamentally that, whereas a bit can only be in one of the available states, a qubit has the possibility of being not only in one of the two basis states but also in any normalized superposition of these:

$$|\psi\rangle = \alpha|0\rangle + \beta|1\rangle, \qquad |\alpha|^2 + |\beta|^2 = 1\,,$$

with the complex coefficients α and β. One of the qubit implementation scenarios (of which there are many) uses the spin $\pm 1/2$ states of a charge carrier (an electron or a hole). For pure quantum-mechanical states, the coefficients α, β and the average projections of the electron spin onto the x-, y-, z-axes of the Cartesian coordinate system are related by the well-known expressions

$$s_x = \mathrm{Re}\,\{\alpha^*\beta\}\,, \quad s_y = \mathrm{Im}\,\{\alpha^*\beta\}\,, \quad s_z = \frac{1}{2}\left(|\alpha|^2 - |\beta|^2\right). \quad (1)$$

The states of a qubit can be described by a vector **s** on the Bloch sphere. A qubit can store much larger amounts of information compared to a bit, the exact amount depending on how accurately the position of the vector **s** is known. Spin-dependent optical and transport phenomena and their practical applications advancing the prospective technologies based on electron spin devices and apparatus are the subject of the field generally known as spintronics. Semiconductor spintronics has as its tasks to study the orientation (injection), accumulation, and detection of spins and their ability to be optically and electrically controlled. While spintronics is currently still in its infancy and in need of new conceptual ideas to realize effective electron spin-based devices, the attractive and exciting world of spin-dependent phenomena is definitely worth exploring and, as is often the case in other fields of physics, basic research will be sooner or later translated into practical applications. This brief report starts with a bird's eye view of spin-dependent phenomena that are explored in the physics of semiconductor nanostructures, followed by a more detailed review of two groups of

E L Ivchenko Ioffe Physical Technical Institute, Russian Academy of Sciences, St. Petersburg, Russian Federation
E-mail: ivchenko@coherent.ioffe.ru

Uspekhi Fizicheskikh Nauk **182** (8) 869 – 900 (2012)
DOI: 10.3367/UFNr.0182.201208f.0869
Translated by E G Strel'chenko, S D Danilov, K A Postnov; edited by A Radzig, A M Semikhatov

Uspekhi Fizicheskikh Nauk **182** (8) 869 – 876 (2012)
DOI: 10.3367/UFNr.0182.201208g.0869
Translated by E G Strel'chenko; edited by A Radzig

phenomena related to the optical control of electron spins in planar arrays of quantum dots and to the magneto-optics of single quantum dots.

2. Problems in spintronics

In this section we consider one by one the problems (illustrated schematically in Fig. 1) whose solution will potentially benefit the practical application of spintronics. Sections 3 to 5 will provide some illustrative examples of how electron spins can currently be controlled.

Effective g factor. This parameter, also know as the Landé factor, is key to describing the interaction of the electron spin with the magnetic field (Zeeman effect). In a typical semiconductor, the effective g factor is highly sensitive to the band gap width and to the valence band spin–orbit splitting. The bulk semiconductor values of the g factor vary from $+2$ to -50. In nanostructures, superlattices, quantum wells, quantum wires, and quantum dots, the g factor is strongly dependent on the shape and geometrical sizes of the nanoobject. In a magnetic field $\mathbf{B}$, the electron spin rotates about the vector $\mathbf{B}$ with an angular velocity $\mathbf{\Omega_B} = g\mu_B\mathbf{B}/\hbar$, where μ_B is the Bohr magneton (Larmor precession).

The theory of the Zeeman effect in heterostructures developed in the 1990s [4] yields the following formula for the transverse electron g factor ($g_{xx} = g_{yy}$) in the lower conduction subband of a quantum well (QW), quantum wire (QWR), and quantum dot (QD) [5]:

$$g = g_0 + \left(g_A(E_{e1}) - g_0\right) w_A + \left(g_B(E_{e1}) - g_0\right) w_B + \left(g_B(E_{e1}) - g_A(E_{e1})\right) V_{3-d}(R) f^2(R)\,. \quad (2)$$

The notation here is as follows: g_0 is the free electron g factor ($g_0 \approx 2$); d is the nanostructure dimensionality ($d = 0, 1, 2$ for a QD, QWR, and QW, respectively); V_n is the generalized volume ($4\pi R_{QD}^3/3$ for a spherical quantum dot of radius R_{QD}, πR_{QWR}^2 for a cylindrical quantum wire of cross-section radius R_{QWR}, and $2R_{QW}$ for a quantum dot of width $a \equiv 2R_{QW}$); A(B) stands for the composite material the well (barrier) is made of; E_{e1} is the dimensional quantization energy of the ground state electron (e1) as counted from the conduction band bottom of material A; w_A (w_B) is the probability of finding the electron in material A (B); $g_A(E) = g(E)$ and $g_B(E) = g(E - \Delta E_c)$:

$$g(E) = g_0 - \frac{4}{3}\frac{|p_{cv}|^2}{m_0}\frac{\Delta}{E_g(E_g + \Delta)} + \Delta g\,; \quad (3)$$

E_g is the band gap width; Δ is the valence band spin–orbit splitting; ΔE_c is the conduction band discontinuity at the A/B interface; $p_{cv} = \langle S|\hat{p}_x|X\rangle$ is the interband matrix element of the momentum operator calculated between the orbital Bloch functions Γ_1 and Γ_{15}; Δg is the remote band contribution to the g factor treated as a small fitting parameter, and, finally, $f(R)$ is the boundary value of the electron envelope wave function.

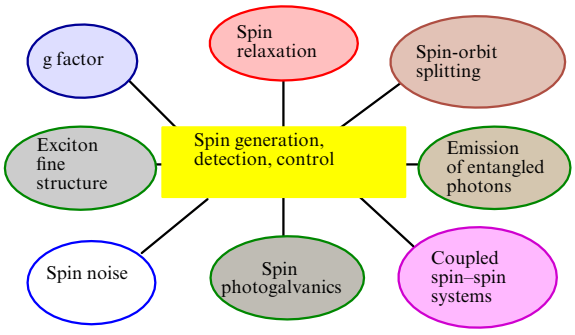

Figure 1. Purposes (center) and problems of spintronics.

Figure 2 reproduces a comparison taken from Ref. [6] of the experimental data on the electron g factor in quantum dot structures with the calculated results based on the theory developed in Refs [4, 5]. The theory of the longitudinal g factor (g_{zz}) of light holes in quantum wells has recently been presented in Ref. [7].

Spin splitting of dimensional quantization subbands. In a d-dimensional medium ($d = 1, 2, 3$) with no inversion center, free carrier states are spin-split. In particular, the effective Hamiltonian for quantum dot electrons in the lower dimensional quantization subband e1 contains, in addition to the standard parabolic dispersion $\hbar^2(k_x^2 + k_y^2)/2m^*$ (m^* is the effective mass), spin-dependent terms linear in the wave vector [8, 9]:

$$\mathcal{H}_{\mathbf{k}}^{(1)} = \beta_{lm}\sigma_l k_m \quad (4)$$

(where σ_l are Pauli matrices), which have the effect that, even in the absence of a magnetic field, the spin of an electron in the state with wave vector $\mathbf{k}$ precesses at an angular frequency $\mathbf{\Omega_k}$ with components $\Omega_{\mathbf{k}l} = 2\beta_{lm}k_m/\hbar$. The fact that the components β_{lm} of the pseudotensor are electric field-dependent allows the spin to be controlled by both a magnetic and an electric field. The theory of the spin splitting of electronic subbands is described in book [10], which also includes a basic bibliography on the topic. In centrosymmetric bulk semiconductors, for example, in Si crystals, symmetry prevents such splitting. However, there is no inversion center in an Si quantum dot with an odd number of atomic planes, so that the splitting is nonzero; the components of the corresponding

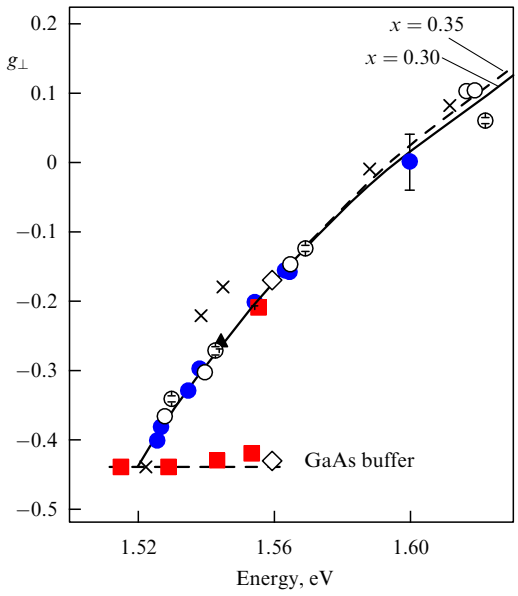

Figure 2. Transverse electron g factor ($g_\perp$) in a GaAs/$Al_xGa_{1-x}As$ quantum dot structure as a function of optical resonance energy. Different symbols refer to experimental values obtained from different samples. Solid and dashed lines were calculated for structure compositions with $x = 0.30$ and $x = 0.35$. Horizontal dashed line points to the electron g factor in a bulk GaAs crystal [6].

tensor β were calculated using the microscopic strong coupling method [11].

Spin relaxation. Spin relaxation time is another key parameter in spintronics. In semiconductor quantum wells, spin relaxation is predominantly via the Dyakonov–Perel mechanism, due to spin precession with angular frequency $\mathbf{\Omega}_{\mathbf{k}}$ (see above). An electron scattering from a state with wave vector $\mathbf{k}$ to that with $\mathbf{k}'$ changes the direction of its axis of rotation, resulting, as the electron undergoes multiple successive collisions, in its spin vector exhibiting random diffusive motion over the Bloch sphere. But this is exactly spin relaxation, because diffusive random walk reduces the average spin value exponentially. Prior to Ref. [12], the corresponding relaxation time was believed to be determined by the transport relaxation time for defect or phonon scattering, i.e. by the mobility-determining time. In Refs [12–14] it was shown that, while electron–electron collisions have no effect on the mobility, they have an effect on the spin relaxation time. Indeed, for an electron to change the direction of its wave vector — and hence the direction of a spin precession axis — it does not matter whether the scattering is by a defect, a phonon, or another electron. As seen from Fig. 3, which compares theoretical and experimental results, the Dyakonov–Perel relaxation is due to electron–electron collisions in perfectly doped quantum well structures at temperatures between 10 K and 100 K.

Fine structure of exciton energy spectrum. What is commonly referred to as a mechanical exciton is a bound electron–hole state calculated by allowing only for the direct pairwise Coulomb interaction in the semiconductor. Because electron (hole) states in a quantum dot are (doubly) spin-degenerate, the ground state of a mechanical exciton is fourfold degenerate. Including the exchange electron–hole interaction removes the degeneracy of the exciton level, at least partially. The theory of the fine structure of exciton states in semiconducting structures can be found in books [10, 15] and review paper [16] (see also original paper [17]). In Section 5, the nanostructure potential shape and the crystallographic orientation of the quantum dot will be discussed in terms of how they affect the splitting behavior of the exciton sublevels, and new experimental and theoretical results will be presented on the spin properties of unstrained GaAs/AlGaAs (111) quantum dots [18].

Emission of entangled photon pairs. In quantum dots possessing D_{2d} (D_{3h}, C_{3v}) symmetry, there is a twofold degeneracy for the exciton sublevels that are optically active in the directions normal to the growth axis. The photoluminescence of biexcitons in such dots allows entangled photon pairs to be generated that are described by the wave function

$$\frac{1}{\sqrt{2}}\left(|\sigma_+\rangle_{\text{biexc}}\,|\sigma_-\rangle_{\text{exc}} + |\sigma_-\rangle_{\text{biexc}}\,|\sigma_+\rangle_{\text{exc}}\right), \qquad (5)$$

where $|\sigma_\pm\rangle_{\text{biexc}}$ is a photon with polarization σ_+ or σ_-, emitted due to biexciton recombination with the production of a photon and an exciton, and $|\sigma_\pm\rangle_{\text{exc}}$ is the second photon emitted on the recombination of the remaining exciton, with

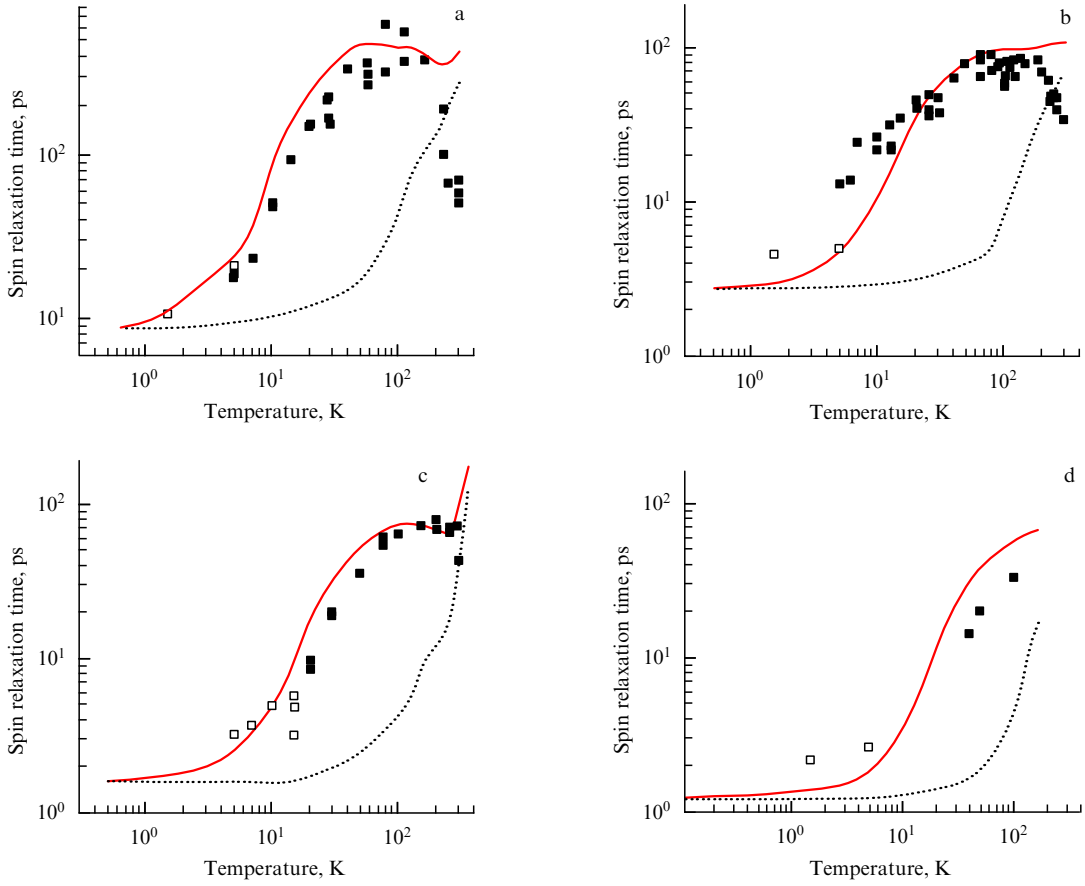

Figure 3. Temperature dependence of an electron spin relaxation time for four GaAs/AlGaAs quantum dot structures with electron concentrations: 1.75×10^{11} cm^{-2} (a), 2.3×10^{11} cm^{-2} (b), 3.1×10^{11} cm^{-2} (c), and 3.3×10^{11} cm^{-2} (d). Experimental results are marked by squares. Solid and dashed lines are calculated, respectively, with and without account for electron–electron collisions. In either case, account was taken of electron scattering by defects and phonons, which is described by the momentum relaxation time τ_p determined independently from transport measurements [14].

polarization being opposite to that of the first photon. Due to the interparticle interaction, the two phonons differ in energy by 1–2 meV and are distinguishable spectroscopically. In quantum dots of lower symmetry, the radiation doublet splits into two linearly polarized dipoles, resulting, if the splitting exceeds the uncertainty $\hbar/\tau$ (τ is the exciton lifetime), in the disappearance of entanglement, i.e. of coherence between the two bracketed states in expression (5). References [19, 20] consider two independent mechanisms, one paramagnetic and one diamagnetic, in which a magnetic field suppresses the original splitting of the radiation doublet.

Coupled spin–spin systems. What in particular distinguishes quantum dots from quantum wells (or wires) is the absence of free two-dimensional (or one-dimensional) motion in them and the fact that the Dyakonov–Perel spin relaxation mechanism does not work. However, with as many as $10^5 - 10^6$ host lattice nuclei in a typical quantum dot, the random nuclear spin exerts influence on the electron spin in this case [21]. Given the optical orientation of the electrons, the nuclear spins can also be polarized, thus giving rise to a coupled spin–spin system, a subject of active research in recent years (see, for example, Refs [22, 23]).

Spin noise. Noise determines the minimum signal amplitudes which can be processed with the means of electronics (in particular, spintronics). Moreover, the study of spin fluctuations provides independent information about the properties of the spin system in equilibrium and nonequilibrium conditions. While fluctuations of the free carrier spin polarization in semiconductors have been under theoretical study since the 1970s [24], it is only relatively recently that spin noise was detected in experiments on semiconductors (see Ref. [25] for a review) — many years, incidentally, after a similar observation in atomic physics back in 1981 [26]. Under equilibrium conditions, the spectral fluctuation density has the Lorentzian form

$$\langle \delta s_i^2 \rangle_\omega = \frac{1}{2} \frac{n\tau_s}{1 + (\omega\tau_s)^2}, \qquad (6)$$

where n is the electron concentration, τ_s is the electron spin relaxation time, and $i = x, y, z$. In a magnetic field $\mathbf{B}$, the spin polarization has its transverse component $\delta\mathbf{s} \perp \mathbf{B}$ fluctuating according to formula (6), with the frequency ω replaced by the difference $\omega - \Omega_\mathbf{B}$. As a result, the spectral peak shifts from point $\omega = 0$ to the Larmor precession frequency $\Omega_\mathbf{B}$, which is exactly what is observed in a 2D electron gas [25]. A similar phenomenon has been observed for an assembly of quantum dots [27]. Some theoretical aspects of spin fluctuations in quantum wires were treated recently in Ref. [28].

Spin photogalvanics. Similar to wheel or propeller rotation converting to translation, gyrotropic media allow the conversion, direct or inverse, of the angular momentum into translational motion. In the electron Hamiltonian, it is the spin-dependent terms linear in $\mathbf{k}$ [see formula (4)] which incorporate this possibility and, hence, account for the circular photogalvanic effect theoretically predicted in Ref. [29] in 1978 (more details are in paper [30] and books [10, 15, 31]).

3. Faraday and Kerr spin effects

Currently, the most popular optical spectroscopy approach to the study of electron spin orientation in nanostructures is to adopt the two-beam pump–probe method. Theoretical paper [32] was apparently the first publication to suggest applying this method to bulk semiconductors. The paper considered

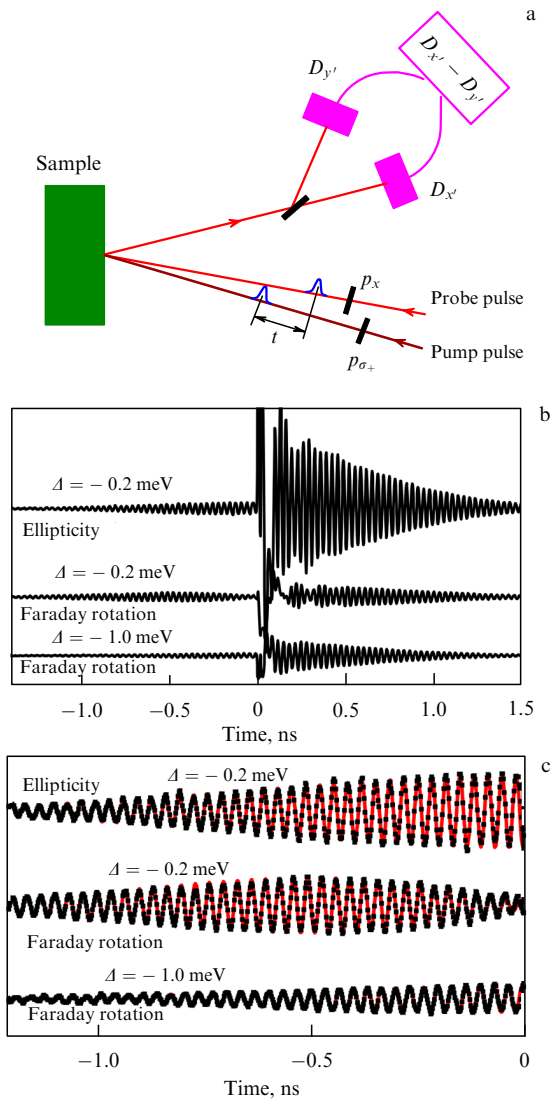

Figure 4. (a) Schematic setup for measuring the rotation angle of the probe beam polarization plane in the spin Faraday effect induced by a circularly polarized pump beam. (b) Ellipticity and Faraday rotation temporal signals measured at near-equal pumping and probing frequencies with mismatch $\Delta \equiv \hbar(\omega_P - \omega_{pr}) = -0.2$ meV and $\Delta = -1$ meV. (c) Comparison of theoretical (solid lines) and experimental (dots) results in the negative time delay range. Note that the dots nearly fit to the curves [33].

two monochromatic beams: one highly intensive and circularly polarized, which is responsible for the optical orientation of electron spins, and the other polarized linearly, which acts as a probe. The aim was to study how the probe beam rotates its polarization plane in the transmission geometry (the so-called Faraday spin effect) or in the reflection geometry (Kerr spin effect) (the magnitude of rotation being proportional to the induced electron spin). The current pump–probe setup uses short, picosecond pulses and measures the angle of rotation θ of the probe pulse polarization plane as a function of the interpulse time delay t (Fig. 4a).

4. Spin synchronization in an assembly of charged quantum dots

Figure 4b shows the beats of the spin Faraday rotation and induced ellipticity signals measured at a temperature of 4 K as a function of time delay t on an array of charged InGaAs/GaAs quantum dots. The sample under study,

subjected to a transverse magnetic field ($B = 4$ T, and Larmor precession period ≈ 33 ps), was periodically excited by short circularly polarized pump pulses at a repetition period $T_R = 13.2$ ns, with the periodic probe pulse train shifted by time t (see Ref. [34]). In the performance of an experiment it was possible to vary the mismatch between the carrying frequencies of the pump pulses (ω_P) and the probe pulses (ω_{pr}). The pump pulse can cause a so-called trion to form in the quantum dot, namely a system of two opposite-spin electrons and a heavy hole. Because the trion recombination time equals ≈ 0.4 ns, most of the time each quantum dot contains one electron, whose optical orientation is precisely what produces the spin Faraday effect. Increasing the delay t decreases the amplitude of the spin beats. The reason for this loss of spin coherence does not relate to the time of the actual spin relaxation, which greatly exceeds the repetition period T_R, but rather is due to the spread in the electron Larmor precession frequencies in the excited quantum dots, whose resonance frequency ω_0 differs from the carrying frequency ω_P by no more than the inverse pulse duration τ_p^{-1}. Surprisingly, at first sight, the occurrence of a signal at negative values of t (Fig. 4b). To describe this unusual effect, a microscopic theory was developed [35] to account for the excitation and measurement of long-lived spin coherence and how to control it in singly charged quantum dots by using short-duration optical pulses in the pump–probe mode. As seen from Fig. 4b, calculations for negative values of t using this theory agree well with the experiment.

The key stages of the theoretical treatment are briefly as follows. The starting point is to find out the effect of a short-duration pulse on a single, charged quantum dot. The resonance approximation yields the following equations:

$$i\hbar\dot{\psi}_{3/2} = \hbar\omega_0\psi_{3/2} + V_+(t)\,\psi_{1/2}\,, \qquad i\hbar\dot{\psi}_{1/2} = V_+^*(t)\,\psi_{3/2}\,,$$

$$i\hbar\dot{\psi}_{-3/2} = \hbar\omega_0\psi_{-3/2} + V_-(t)\,\psi_{-1/2}\,, \quad i\hbar\dot{\psi}_{-1/2} = V_-^*(t)\,\psi_{-3/2}\,.$$

Here, $\psi_{\pm 1/2}$ and $\psi_{\pm 3/2}$ are the respective detection probability amplitudes of a single spin $\pm 1/2$ electron or a hole spin $\pm 3/2$ trion in the quantum dot, $V_\pm(t) = -\int d(\mathbf{r})\,E_{\sigma^\pm}(\mathbf{r},t)\,d^3r$ are the interaction matrix elements with the electric field $E_{\sigma^\pm}(\mathbf{r},t)$ of the right and left circularly polarized light wave, and $\dot{\psi} \equiv \partial\psi/\partial t$. The optical transition dipole moment, a quantity characterizing the efficiency of interaction, is given by

$$d(\mathbf{r}) = -i\,\frac{ep_{cv}}{\omega_0 m_0}\,F(\mathbf{r},\mathbf{r})\,, \tag{7}$$

where e is the electron charge, and m_0 is the free electron mass. The two-particle envelope F is defined as

$$F(\mathbf{r},\mathbf{r}) = \varphi_h(\mathbf{r})\,\varphi_e^{(tr)}(\mathbf{r})\int d^3r'\varphi_e(\mathbf{r}')\,\varphi_e^{(tr)}(\mathbf{r}')\,, \tag{8}$$

where $\varphi_e^{(tr)}$ and φ_h are the electron and hole one-particle enveloping functions in the trion, respectively, and φ_e is the envelope of the single (resident) electron in the quantum dot.

The spin $\mathbf{S}^+$ of an electron after being acted by the pump pulse is related linearly to the spin $\mathbf{S}^-$ at the moment when the pulse with polarization σ_+ arrives:

$$S_\alpha^+ = \mathcal{L}_{\alpha\beta}S_\beta^- + \frac{Q^2-1}{4}\,\delta_{\alpha z}\,,$$

$$\hat{\mathcal{L}} = \begin{bmatrix} Q\cos\Phi & Q\sin\Phi & 0 \\ Q\cos\Phi & -Q\sin\Phi & 0 \\ 0 & 0 & \dfrac{Q^2+1}{2} \end{bmatrix}. \tag{9}$$

For rectangular pulses with $f(t) \equiv V_\pm(t)\exp(i\omega_P t)/\hbar = f_0$ for $|t| < \tau_p/2$, and $f(t) = 0$ outside this interval, we obtain

$$Q = \sqrt{1 - \frac{\Theta^2}{x^2}\sin^2\frac{x}{2}}\,, \qquad \Phi = \pi y - \phi\,, \tag{10}$$

where $\Theta = 2f_0\tau_p$, $x = \sqrt{(2\pi y)^2 + \Theta^2}$ is the effective Rabi frequency, $y = (\omega_P - \omega_0)\,\tau_p/2\pi$ is the dimensionless frequency mismatch, and $\sin\phi = (y/Qx)\sin(x/2)$. In a magnetic field $\mathbf{B} \parallel x$, the transverse spin components oscillate: $S_\beta(\Delta t) = \mathcal{M}_{\beta\gamma}(\Delta t)\,S_\gamma^+$, where the time Δt is measured from the moment at which one of the periodic pump pulses arrives, and where the nonzero components of the matrix $\mathcal{M}$ have the form $\mathcal{M}_{yy} = \mathcal{M}_{zz} = \cos(\Omega_B\Delta t)$, $\mathcal{M}_{zy} = -\mathcal{M}_{yz} = \sin(\Omega_B\Delta t)$, and $\mathcal{M}_{xx} = 1$. As a result, the following closed linear equation can be utilized to find the stationary value of the vector $\mathbf{S}^+$:

$$S_\alpha^+ = \mathcal{L}_{\alpha\beta}\,\mathcal{M}_{\beta\gamma}(T_R)\,S_\gamma^+ + \delta_{\alpha z}\,\frac{Q^2-1}{4}\,.$$

A similar computation yields the probability amplitude corrections $\delta\psi_{\pm 1/2}$, $\delta\psi_{\pm 3/2}$ linear in the probe pulse electric field, thus allowing the angle of rotation θ to be calculated by first finding the spin-dependent amplitude corrections for the transmitted (or reflected) probe pulse and then summing them over the quantum dots.

Quantum dots with a Larmor precession period that is a multiple of T_R, i.e. $\Omega_B T_R = 2\pi N$ (where N is an integer), exhibit a resonant accumulation of spin and contribute dominantly to the spin Faraday rotation. Due to the spread in the frequency Ω_B, the commensurability condition is satisfied by quantum dots with N's differing by ± 1, ± 2, ... Thus, the attenuation of the signal upon increasing $t > 0$ is due to the fact that in quantum dots with different values of N, electron spins rotate with different angular velocities. However, by the time of the arrival of the next pump pulse, the spins steadily align themselves along the z-axis. This phenomenon is similar to the synchronization of laser modes [36].

5. Spectroscopy of single quantum dots

In a quantum dot grown along the [001]-axis and characterized by the point symmetry C_{2v}, the electron and hole ground states transform according to the equivalent spinor representations Γ_5 (or, in an alternative notation, E'). In the absence of exchange interaction, the ground state of an exciton e1 – hh1 is fourfold degenerate [37]. The exchange interaction between an electron and a hole removes the degeneracy completely and leads to the splitting of the exciton level to the sublevels Γ_1, Γ_2, Γ_3, Γ_4 (or, accordingly, A_1, B_1, A_2, B_2 in other notations of irreducible representations). In Cartesian coordinates ($x_1 \parallel [1\bar{1}0], y_1 \parallel [110], z \parallel [001]$), the states Γ_2 and Γ_4 are optically active for $\mathbf{e} \parallel x_1$ and $\mathbf{e} \parallel y_1$ polarizations, whereas transitions to the other two states, Γ_1 and Γ_3, are forbidden for $\mathbf{e} \perp z$. In a longitudinal magnetic field $\mathbf{B} \parallel z$, the pair of states Γ_1, Γ_3 undergoes mixing, as does the pair Γ_2, Γ_4 — but there is no mixing between the pairs of sublevels. Therefore, the absorption or emission spectra exhibit two lines linearly polarized in the absence of a magnetic field, and circularly polarized in a strong longitudinal magnetic field. For a similar reason, only two of each four processes $(X^-, j) \to (e1, s)$ and $(X^+, s) \to (hh1, j)$ are permitted in

the radiative recombination of a trion X^- (two singlet-state electrons and a heavy hole) or a trion X^+ (two singlet-state holes and an electron) in an external longitudinal magnetic field, so that the emission spectrum exhibits doublets, not quartets. Here, s, j are the indices of the split Zeeman sublevels of a trion or a single carrier in a quantum dot.

GaAs/AlGaAs quantum dots grown along (111) direction obey totally different selection rules. Figure 5 displays the photoluminescence spectrum of an individual quantum dot for stationary over-barrier optical excitation. In this case, time-integrated spectra contain both emission lines of neutral excitons X^0 and those of trions X^- and X^+. As seen from the figure, in a longitudinal magnetic field $\mathbf{B}\|[111]$, instead of doublets comprising circularly polarized σ_+ and σ_- lines, one observes a quartet, two lines of which are right-hand circularly polarized, σ_+, the other two being left-hand circularly polarized, σ_-. The fact that quantum dots grown along [001]- and [111]-axes differ in the structure of their photoluminescence spectra is naturally explained by the difference in their symmetry point groups C_{2v} and C_{3v}. It should be remembered that in the C_{2v} group the heavy hole states $|\pm 3/2\rangle$ transform according to the two-dimensional irreducible representation Γ_5, and the direct product $\Gamma_5 \times \Gamma_5^* = \Gamma_1 + \Gamma_2 + \Gamma_3 + \Gamma_4$ contains only one representation Γ_3, according to which the magnetic field component B_z transforms. In C_{3v}, the states $|\pm 3/2\rangle$ form the basis of the reducible representation $\mathcal{D} = \Gamma_5 + \Gamma_6$, and the direct product $\mathcal{D} \times \mathcal{D}^* = 2\Gamma_1 + 2\Gamma_2$ includes two representations Γ_2, according to which the component $B_{z'}$ ($z' \| [111]$) transforms in this group. As a result, the Zeeman Hamiltonian in the field $\mathbf{B}\|[111]$ is described by two linearly independent parameters g_{h1}, g_{h2}, and the basis $|\pm 3/2\rangle$ has the form of a 2×2 matrix:

$$\mathcal{H}_\mathbf{B} = \frac{1}{2}\,\mu_B\, B_{z'} \begin{bmatrix} g_{h1} & g_{h2} \\ g_{h2} & -g_{h1} \end{bmatrix}. \tag{11}$$

The eigenvalues of the matrix (11) are given by

$$E_\pm = \pm g_h\, \mu_B\, B_{z'}, \quad g_h \equiv \sqrt{g_{h1}^2 + g_{h2}^2}, \tag{12}$$

and the corresponding eingenfunctions can be reduced to the form

$$|h, +\rangle = C_1 \left|\frac{3}{2}\right\rangle + C_2 \left|-\frac{3}{2}\right\rangle,$$

$$|h, -\rangle = -C_2 \left|\frac{3}{2}\right\rangle + C_1 \left|-\frac{3}{2}\right\rangle$$

with the coefficients

$$C_1 = \sqrt{\frac{1}{2}\left(1 + \frac{g_{h1}}{\sqrt{g_{h1}^2 + g_{h2}^2}}\right)},$$

$$C_2 = \mathrm{sign}\,(g_{h2}) \sqrt{\frac{1}{2}\left(1 - \frac{g_{h1}}{\sqrt{g_{h1}^2 + g_{h2}^2}}\right)}.$$

It should be noted that the coefficients C_1, C_2 are independent of the magnetic field. For $C_2 \neq 0$, a spin 1/2 (or $-1/2$) electron can recombine both with a hole $|h, +\rangle$ and with a hole $|h, -\rangle$ to emit a σ_- (or σ_+) photon. Thus, all

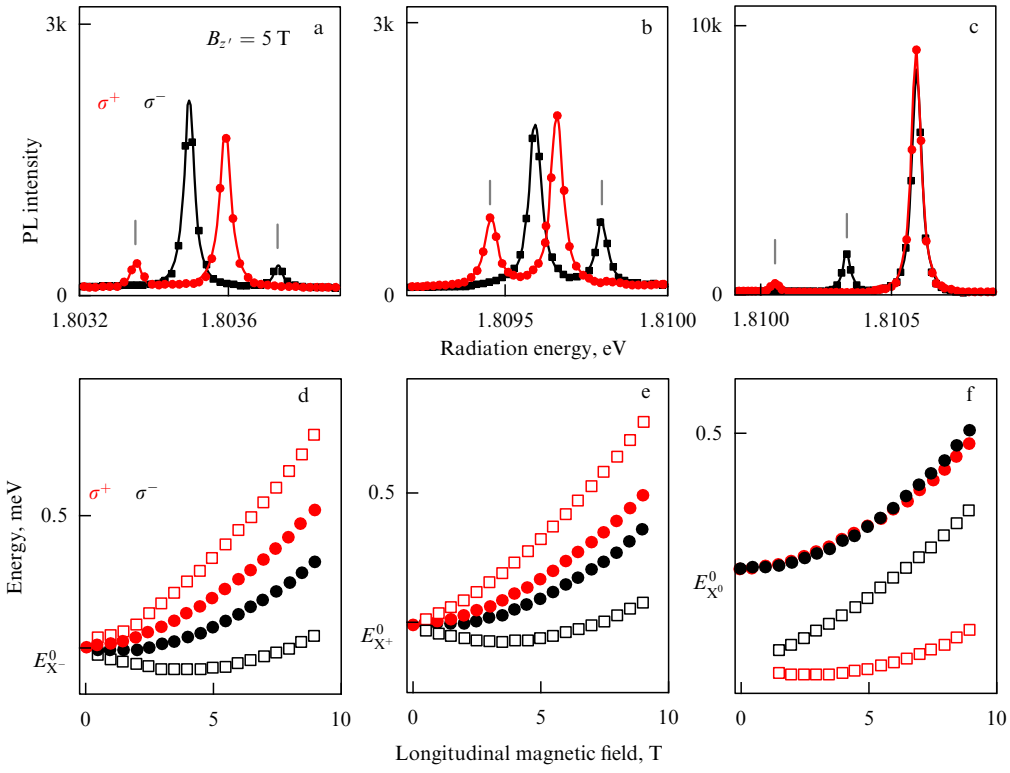

Figure 5. Photoluminescence (PL) spectrum of a single GaAs/AlGaAs (111) quantum dot measured in a magnetic field $B_{z'} = 5$ T in the emission range of trion X^+ (a), trion X^- (b), and neutral exciton X^0 (c); k is taken as a conditional intensity measurement unit. Circles and squares show the right and left circularly polarized emission lines, respectively. (d–f) Change in the position of the corresponding emission line with increasing magnetic field [18].

four transitions turn out to be optically active, whereas in (001) quantum dots the parameter g_{h2} is zero, implying that $C_2 \equiv 0$ and that only two recombination processes are allowed. It should be emphasized that the mixing effect of $\pm 3/2$ states in a longitudinal magnetic field can show its worth in trigonal systems with arbitrary dimensionality $d = 0-3$, including an exciton in Ge crystals formed by an L-valley electron and a Γ_8^+ hole and bound on a neutral donor [38].

A nonzero value g_{h2} of the g factor can be obtained by noting that in bulk zinc blende lattice semiconductors the Zeeman interaction of Γ_8 holes with a magnetic field is described by the Hamiltonian

$$\mathcal{H}_{\mathbf{B}}^{(\Gamma_8)} = -2\mu_{\mathrm{B}}\left[\kappa \mathbf{J}\,\mathbf{B} + q(J_x^3 B_x + J_y^3 B_y + J_z^3 B_z)\right], \quad (13)$$

which contains two dimensionless coefficients, κ and q. Here, x, y and z are the crystallographic axes [100], [010] and [001], and J_x, J_y, and J_z are the angle momentum matrices in the Γ_8 basis. Let us go over in Hamiltonian (13) to the coordinates $x' \| [11\bar{2}]$, $y' \| [\bar{1}10]$, $z' \| [111]$ and introduce the basis functions $|3/2\rangle'$, $|-3/2\rangle'$, which transform according to the reducible representation $\mathcal{D} = \Gamma_5 + \Gamma_6$ of the C_{3v} group. Then, the Zeeman splitting in the field $\mathbf{B} \| [111]$ will be described by a 2×2 matrix with $g_{h1} = -6\kappa$, and $g_{h2} = 2\sqrt{2}q$.

Acknowledgments. This work was supported by an RAS Presidium Program and by RFBR grants. The author is grateful to M M Glasov for helpful discussions of the manuscript.

References

1. Dyakonov M I (Ed.) *Spin Physics in Semiconductors* (Berlin: Springer, 2008)
2. Kusrayev Yu, Landwehr G (Guest Eds) *Semicond. Sci. Technol.* **23** (11) (2008), Special issue on optical orientation
3. *Fiz. Tekh. Poluprovodn.* **42** (8) (2008) [*Semicond.* **42** (8) (2008)], Vladimir Idelevich Perel' (on the 80th anniversary of his birthday), Special issue
4. Ivchenko E L, Kiselev A A *Fiz. Tekh. Poluprovodn.* **26** 1471 (1992) [*Sov. Phys. Semicond.* **26** 827 (1992)]
5. Kiselev A A, Ivchenko E L, Rössler U *Phys. Rev. B* **58** 16353 (1998)
6. Yugova I A et al. *Phys. Rev. B* **75** 245302 (2007)
7. Durnev M V, Glazov M M, Ivchenko E L *Physica E* **44** 797 (2012); arXiv:1111.6837
8. Rashba E I *Fiz. Tverd. Tela* **2** 1224 (1960) [*Sov. Phys. Solid State* **2** 1109 (1960)]
9. Bychkov Yu A, Rashba E I *Pis'ma Zh. Eksp. Teor. Fiz.* **39** 66 (1984) [*JETP Lett.* **39** 78 (1984)]
10. Ivchenko E L *Optical Spectroscopy of Semiconductor Nanostructures* (Harrow, UK: Alpha Sci. Intern. Ltd, 2005)
11. Nestoklon M O, Golub L E, Ivchenko E L *Phys. Rev. B* **73** 235334 (2006)
12. Glazov M M, Ivchenko E L *Pis'ma Zh. Eksp. Teor. Fiz.* **75** 476 (2002) [*JETP Lett.* **75** 403 (2002)]
13. Glazov M M, Ivchenko E L *Zh. Eksp. Teor. Fiz.* **126** 1465 (2004) [*JETP* **99** 1279 (2004)]
14. Leyland W J H et al. *Phys. Rev. B* **75** 165309 (2007)
15. Ivchenko E L, Pikus G E *Superlattices and other Heterostructures*: *Symmetry and Optical Phenomena* (Berlin: Springer-Verlag, 1995); *Superlattices and other Heterostructures*: *Symmetry and Optical Phenomena* 2nd ed. (Berlin: Springer, 1997)
16. Ivchenko E L *Phys. Status Solidi A* **164** 487 (1997)
17. Gupalov S V, Ivchenko E L, Kavokin A V *Zh. Eksp. Teor. Fiz.* **113** 703 (1998) [*JETP* **86** 388 (1998)]
18. Sallen G et al. *Phys. Rev. Lett.* **107** 166604 (2011)
19. Stevenson R M et al. *Phys. Rev. B* **73** 033306 (2006)
20. Glazov M M et al. *Phys. Rev. B* **76** 193313 (2007)
21. Kusrayev Yu G *Usp. Fiz. Nauk* **180** 759 (2010) [*Phys. Usp.* **53** 725 (2010)]
22. Glazov M M, Yugova I A, Efros Al L *Phys. Rev. B* **85** 041303(R) (2012); arXiv:1103.3249
23. Glazov M M *Fiz. Tverd. Tela* **54** 3 (2012) [*Phys. Solid State* **54** 1 (2012)]
24. Ivchenko E L *Fiz. Tekh. Poluprovodn.* **7** 1489 (1973) [*Sov. Phys. Semicond.* **7** 998 (1973)]
25. Müller G M et al. *Physica E* **43** 569 (2010)
26. Aleksandrov E B, Zapasskii V S *Zh. Eksp. Teor. Fiz.* **81** 132 (1981) [*Sov. Phys. JETP* **54** 64 (1981)]
27. Crooker S A et al. *Phys. Rev. Lett.* **104** 036601 (2010)
28. Glazov M M, Sherman E Ya *Phys. Rev. Lett.* **107** 156602 (2011)
29. Ivchenko E L, Pikus G E *Pis'ma Zh. Eksp. Teor. Fiz.* **27** 640 (1978) [*JETP Lett.* **27** 604 (1978)]
30. Ivchenko E L *Usp. Fiz. Nauk* **172** 1461 (2002) [*Phys. Usp.* **45** 1299 (2002)]
31. Ivchenko E L, Ganichev S D, in *Spin Physics in Semiconductors* (Ed. M I Dyakonov) (Berlin: Springer, 2008) p. 245
32. Aronov A G, Ivchenko E L *Fiz. Tverd. Tela* **15** 231 (1973) [*Sov. Phys. Solid State* **15** 160 (1973)]
33. Glazov M M et al. *Phys. Rev. B* **82** 155325 (2010)
34. Greilich A et al. *Science* **313** 341 (2006)
35. Yugova I A et al. *Phys. Rev. B* **80** 104436 (2009)
36. Haken H *Light* Vol. 2 *Laser Light Dynamics* (Amsterdam: North-Holland, 1985) [Translated into Russian (Moscow: Mir, 1988)]
37. Dzhioev R I et al. *Pis'ma Zh. Eksp. Teor. Fiz.* **65** 766 (1997) [*JETP Lett.* **65** 804 (1997)]
38. Averkiev N S et al. *Fiz. Tverd. Tela* **23** 3117 (1981) [*Sov. Phys. Solid State* **23** 1815 (1981)]

PACS numbers: 72.25.Hg, 72.25.Pn, 72.25.Rb, 73.63.Hs
DOI: 10.3367/UFNe.0182.201208h.0876

Spin transport in heterostructures

L E Golub

1. Introduction. Spin splittings

In the absence of an external magnetic field, electronic states can be spin-split if the system has no space inversion center. The reason for these spin splittings is the spin–orbit interaction. The simplest example of a noncentrosymmetric medium is a surface. The Hamiltonian of the spin-orbit interaction in a half-infinite medium assumes the following (Rashba [1, 2]) form:

$$H_{\mathrm{so}} = \alpha(\boldsymbol{\sigma} \times \mathbf{k})\,\mathbf{n}\,. \quad (1)$$

Here, the vector $\boldsymbol{\sigma}$ is composed of Pauli matrices, $\mathbf{k}$ is the electron wave vector, α is a certain number, and $\mathbf{n}$ is a unit normal vector to the surface. This form of such spin–orbit interaction occurs in various noncentrosymmetric semiconductors, metals, and superconductors.

L E Golub Ioffe Physical Technical Institute,
Russian Academy of Sciences, St. Petersburg, Russian Federation
E-mail:golub@coherent.ioffe.ru

Uspekhi Fizicheskikh Nauk **182** (8) 876 – 879 (2012)
DOI: 10.3367/UFNr.0182.201208h.0876
Translated by E G Strel'chenko; edited by A Radzig